DE GRUYTER
OPEN

10.1515/tvsb-2015-0001

Transactions of the VŠB – Technical University of Ostrava

No. 1, 2015, Vol. 15, Civil Engineering Series

paper #01

Ivan BALÁZS[1], Jindřich MELCHER[2]

STABILITY OF THIN-WALLED BEAMS WITH LATERAL CONTINUOUS RESTRAINT

Abstract

Metal beams of thin-walled cross-sections have been widely used in building industry as members of load-bearing structures. Their resistance is usually limited by lateral torsional buckling. It can be increased in case a beam is laterally supported by members of cladding or ceiling construction. The paper deals with possibilities of determination of critical load of thin-walled beams with lateral continuous restraint which is crucial for beam buckling resistance assessment.

Keywords

Critical load, finite difference method, lateral torsional buckling, numerical analysis, stability, thin-walled beam.

1 INTRODUCTION

Resistance of slender metal beams of thin-walled cross-sections with no lateral restraints is usually limited by lateral torsional buckling. In case they are utilized as purlins or girts, members of roof or wall cladding can be attached to them. It results in lateral restraint that prevents displacement of the beam cross-section and therefore contributes to its buckling resistance. If it is correctly taken into account, more economical design of the cross-section can be achieved. The paper focuses on possibilities of determination of critical load of thin-walled metal beams with lateral continuous restraint. A numerical method for critical load computation is described and results are compared with results obtained using software based on finite element method.

2 LATERAL TORSIONAL BUCKLING OF AN IDEAL BEAM WITHOUT LATERAL RESTRAINTS

Lateral torsional buckling of an ideal beam (with no initial imperfection) with no lateral restraints is characterized by deformation of the member cross-section consisting of two components – lateral displacement of the cross-section out of plane of bending v and angle of rotation φ [1]. For a beam of monosymmetric cross-section this effect is illustrated in Fig. 1 where q_z is vertical load (in the XZ plane), C_g indicates cross-section center of gravity, C_s cross-section shear center, a_z distance of center of gravity and shear center and e_z distance of the position of load application and center of gravity. Compressed part of the cross-section tends to buckle out of plane of bending.

Lateral torsional buckling of an ideal beam occurs when critical moment M_{cr} (caused by critical load) is reached. The problem of stability of an arbitrary thin-walled member of open cross-section in bending and compression is defined by Vlasov in form of differential equations [1].

[1] Ing. Ivan Balázs, Institute of Metal and Timber Structures, Faculty of Civil Engineering, Brno University of Technology, Veveří 331/95, 602 00 Brno, Czech Republic, phone: (+420) 541 147 329, e-mail: balazs.i@fce.vutbr.cz.

[2] Prof. Ing. Jindřich Melcher, DrSc., Institute of Metal and Timber Structures, Faculty of Civil Engineering, Brno University of Technology, Veveří 331/95, 602 00 Brno, Czech Republic, phone: (+420) 541 147 300, e-mail: melcher.j@fce.vutbr.cz.

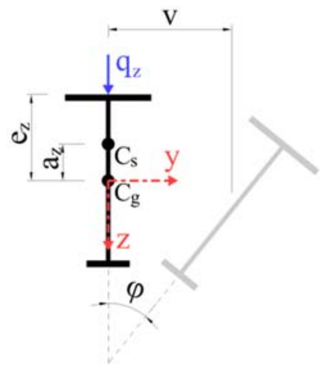

Fig. 1: Lateral torsional buckling of an ideal beam

After modification for case of a member in bending only the problem is defined by two homogenous differential equations of fourth order (1) and (2) and appropriate boundary conditions [1]. For a member simply supported in bending as well as in torsion boundary conditions (3) apply, for a fixed member boundary conditions (4) apply [1].

$$EI_z v^{IV} + (M_y \varphi)'' = 0\,, \tag{1}$$

$$EI_\omega \varphi^{IV} - GI_t \varphi'' - 2b_z (M_y \varphi)' + q_z (e_z - a_z)\varphi + M_y v'' = 0\,, \tag{2}$$

$$v(0) = v(L) = 0, v''(0) = v''(L) = 0, \varphi(0) = \varphi(L) = 0, \varphi''(0) = \varphi''(L) = 0, \tag{3}$$

$$v(0) = v(L) = 0, v'(0) = v'(L) = 0, \varphi(0) = \varphi(L) = 0, \varphi'(0) = \varphi'(L) = 0, \tag{4}$$

where E is modulus of elasticity, G shear modulus of elasticity, I_z second moment of area, I_ω warping constant, I_t torsion constant, q_z vertical load (in the XZ plane), M_y bending moment, v and φ unknown functions of deformation and b_z is Wagner coefficient. The expression for its determination can be found e.g. in [1]. Actual standard for design of steel structures [3] indicates it as z_j.

In the mathematical point of view the critical load is given as eigenvalue problem of differential equations (1) and (2) with appropriate boundary conditions. Derived expression for critical moment of an isolated beam (with no lateral restraint) of at least monosymmetric cross-section loaded by a load that crosses its shear center can be found in the standard [3].

3 LATERAL TORSIONAL BUCKLING OF AN IDEAL BEAM WITH LATERAL CONTINUOUS RESTRAINT

Let us consider that there is lateral continuous restraint located in a distance of c_z from the cross-section center of gravity (at the point C_{lat}) that prevents lateral displacement of the cross-section. Therefore rotation of the cross-section around fixed axis occurs [1]. The situation can be seen in Fig. 2.

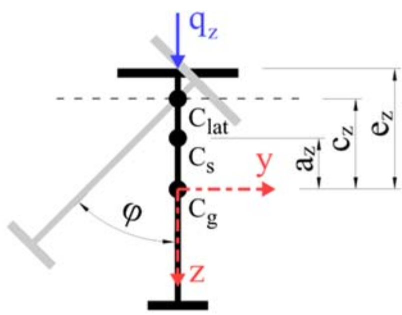

Fig. 2: Lateral torsional buckling of an ideal beam with lateral restraint

The lateral restraint is considered to be perfectly rigid. The beam span is L. An ideal beam is considered (with no initial imperfections).

3.1 Critical load determination

Since lateral displacement of the cross-section is prevented, the only unknown function of deformation is angle of rotation φ and differential equations (1) and (2) are modified accordingly. It results in one homogenous differential equation of order four (5) [1] (in general with nonconstant coefficients) with boundary conditions (6) for simply supported beam and (7) for fixed beam:

$$\left[EI_\omega + EI_z(c_z - a_z)^2\right]\varphi^{IV} - GI_t\varphi'' + 2(c_z - a_z - b_z)(M_y\varphi')' + q_z(e_z - c_z)\varphi = 0\,, \tag{5}$$

$$\varphi(0) = \varphi(L) = 0, \varphi''(0) = \varphi''(L) = 0\,, \tag{6}$$

$$\varphi(0) = \varphi(L) = 0, \varphi'(0) = \varphi'(L) = 0\,, \tag{7}$$

where q_z is the magnitude of load at bifurcation of equilibrium (critical load). In the mathematical point of view it is an eigenvalue problem. In this case it is the so called Sturm-Liouville eigenvalue problem of differential equation of fourth order [4]. Solution of this complex problem is possible using combination of selected numerical methods, e.g. finite difference method and inverse power method. Both methods are easily algorithmizable. The procedure of the methods is described.

Equation (5) is transformed to the form (8):

$$A\varphi^{IV} - B\varphi'' + CM'_y\varphi'' = q_z D\varphi\,, \tag{8}$$

where

$$A = \left[EI_\omega + EI_z(c_z - a_z)^2\right], \tag{9}$$

$$B = GI_t\,, \tag{10}$$

$$C = 2(c_z - a_z - b_z)\,, \tag{11}$$

$$D = (c_z - e_z)\,. \tag{12}$$

Equation (8) will be used as initial for eigenvalue problem solution (critical load determination). The interval <0; L> (beam span) is divided into N subintervals using a step of h and $N - 1$ equidistant nodes x_i in such a way that $0 = x_0 < x_1 < \ldots < x_{N-1} < x_N = L$, where $x_i = ih$ and $h = 1 / N$ (Fig. 3). Certain value of the function φ is assigned to each node x_i. It arises from the boundary conditions (6) and (7) that $\varphi_0 = \varphi(0) = 0$ and $\varphi_N = \varphi(L) = 0$.

Let us introduce first (13), second (14) and fourth (15) central difference for first, second and fourth derivative approximation:

$$f'_i = \frac{\varphi_{i+1} - \varphi_{i-1}}{2h}\,, \tag{13}$$

$$f''_i = \frac{\varphi_{i+1} - 2\varphi_i + \varphi_{i-1}}{h^2}\,, \tag{14}$$

$$f_i^{IV} = \frac{\varphi_{i+2} - 4\varphi_{i+1} + 6\varphi_i - 4\varphi_{i-1} + \varphi_{i-2}}{h^4}\,. \tag{15}$$

Application of the central differences to nodes x_0 and x_N requires functional values in fictitious nodes $x_{-1} = -h$ and $x_{N+1} = L + h$. It is possible to determine the functional values φ_{-1} and φ_{N+1} using boundary conditions. For simply supported beam application of boundary conditions (6) results in functional values $\varphi_{-1} = -\varphi_1$ and $\varphi_{N+1} = -\varphi_{N-1}$. For fixed beam application of (7) results in functional values $\varphi_{-1} = \varphi_1$ and $\varphi_{N+1} = \varphi_{N-1}$. Functional values at nodes from x_1 to x_{N-1} are to be solved.

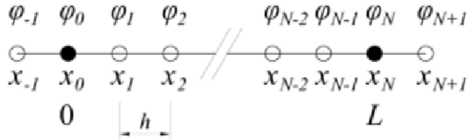

Fig. 3: Difference scheme

For each node x_i, where $i = 1, \ldots, N - 1$ equation (16) is assembled putting central differences (14) and (15) into equation (8) instead of second and fourth derivatives:

$$A\varphi_i^{IV} - B\varphi_i'' + CM'_{yi}\varphi_i'' = q_z D\varphi_i \,, \tag{16}$$

This modification leads to a system of $N - 1$ algebraic equations that can be expressed as follows (17):

$$\begin{vmatrix} K_{11} & K_{12} & K_{13} & & & & & & \\ K_{21} & K_{22} & K_{23} & \ldots & & & & & \\ K_{31} & K_{32} & K_{33} & \ldots & \ldots & & & & \\ & K_{42} & K_{43} & \ldots & \ldots & \ldots & & & \\ & & K_{53} & \ldots & \ldots & \ldots & K_{N-5,N-3} & & \\ & & & \ldots & \ldots & \ldots & K_{N-4,N-3} & K_{N-4,N-2} & \\ & & & & \ldots & \ldots & K_{N-3,N-3} & K_{N-3,N-2} & K_{N-3,N-1} \\ & & & & & \ldots & K_{N-2,N-3} & K_{N-2,N-2} & K_{N-3,N-1} \\ & & & & & & K_{N-1,N-3} & K_{N-1,N-2} & K_{N-3,N-1} \end{vmatrix} \begin{vmatrix} \varphi_1 \\ \varphi_2 \\ \varphi_3 \\ \ldots \\ \ldots \\ \ldots \\ \varphi_{N-3} \\ \varphi_{N-2} \\ \varphi_{N-1} \end{vmatrix} = q_z D h^4 \begin{vmatrix} \varphi_1 \\ \varphi_2 \\ \varphi_3 \\ \ldots \\ \ldots \\ \ldots \\ \varphi_{N-3} \\ \varphi_{N-2} \\ \varphi_{N-1} \end{vmatrix} \tag{17}$$

Individual members of the system matrix are defined by following expressions:

$$K_{i+2,i} = K_{i,i+2} = A \text{ for } i = 1, \ldots, N - 3, \tag{18}$$

$$K_{i+1,i} = -4A + S_{i+1} \text{ for } i = 1, \ldots, N - 2, \tag{19}$$

$$K_{i,i+1} = -4A + S_i \text{ for } i = 1, \ldots, N - 2, \tag{20}$$

$$K_{i,i} = 6A - 2S_i \text{ for } i = 2, \ldots, N - 2. \tag{21}$$

For members $K_{1,1}$ and $K_{N-1,N-1}$ boundary conditions at nodes $x_0 = 0$ and $x_N = L$ have to be taken into account. For a simply supported beam expression (22) applies, for a fixed beam expression (23) applies.

$$K_{i,i} = 5A - 2S_i \text{ for } i = \{1; N - 1\}, \tag{22}$$

$$K_{i,i} = 7A - 2S_i \text{ for } i = \{1; N - 1\}. \tag{23}$$

Expression S_i is defined as follows (24):

$$S_i = h^2 (CM'_{yi} - B) \cdot \tag{24}$$

System of algebraic equations (17) can be expressed as follows (bold letters indicate vectors):

$$K\,\boldsymbol{\varphi} = \mathrm{q}_z\, D\, h^4\, \boldsymbol{\varphi} \,, \tag{25}$$

where

$$\boldsymbol{\varphi} = |\ \varphi_1 \quad \varphi_2 \quad \varphi_3 \quad \ldots \quad \varphi_{N-3} \quad \varphi_{N-2} \quad \varphi_{N-1}\ |^{\mathrm{T}}. \tag{26}$$

It can be modified to form (27):

$$G\,\boldsymbol{\varphi} = q_z\, \boldsymbol{\varphi} \,, \tag{27}$$

where the matrix G is defined as expression (28):

$$G = \frac{K}{Dh^4} \cdot \tag{28}$$

For the eigenvalue problem solution (critical load q_z determination) equation (27) is utilized. For practical purposes the most important is the minimum positive eigenvalue [5] (the lowest load that causes lateral torsional buckling of an ideal beam).

Approximation of the minimum eigenvalue and appropriate eigenvector (buckling shape) of the matrix G can be computed e.g. using inverse power method [6] (power method applied to the matrix G^{-1}). The algorithm of the power method can be found e.g. in [6]. Another possibility is application of the iterative QR algorithm [7] that gives all the eigenvalues with appropriate eigenvectors of the matrix G (complete eigenvalue problem solution). The algorithm is briefly outlined [7]:

$$G = G_0 = Q_0 R_0 , \tag{29}$$

$$G_{k+1} = R_k Q_k , k \geq 1 , \tag{30}$$

where matrices Q_k and R_k are products of the so called QR decomposition of the matrix G_k. It is possible to decompose the matrix G_k to matrices Q_k and R_k e.g. using Gram-Schmidt orthonormalization process [8]. Expression (31) then applies:

$$\lim_{k \to \infty} G_k = E , \tag{31}$$

where E is a diagonal matrix with eigenvalues located on its diagonal (other members are equal to zero). The eigenvectors (buckling shapes) are given as columns of a matrix resulting from matrix Q_{k+1} and Q_k multiplication.

3.2 Example of the critical load calculation

For the example of the critical load calculation a steel beam of double symmetric cross-section according to Fig. 4 is chosen. There is lateral continuous restraint located at a distance of c_z = 50 mm from the center of gravity.

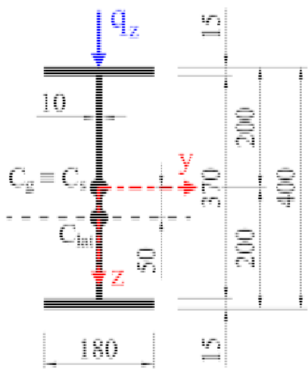

Fig. 4: Cross-section of the investigated beam

The beam span is L = 5 m. There is vertical uniformly distributed load of a magnitude of 1 kN/m acting at the top flange. Two types of support conditions according to boundary conditions (6) and (7) are considered.

The procedure explained in section 3.1 with a step of h = 0,10 m (number of subintervals N = 50) is applied. The solution leads to differential equation (32) with boundary conditions (6) or (7), respectively:

$$121122{,}3\varphi^{IV} - 41848{,}8\varphi'' + 0{,}1M'_y\varphi'' = 0{,}25q_z\varphi , \tag{32}$$

which is transformed to a system of 49 algebraic equations using finite difference method and solved by inverse power method. It results in minimum eigenvalue of 145520 (simply supported beam) and

472480 (fixed beam). In the physical point of view these values represent critical loads (in N/m). The appropriate critical moments are calculated using (33) for simply supported beam and (34) for fixed beam:

$$M_{cr} = \frac{1}{8} q_{cr} L^2 , \tag{33}$$

$$M_{cr} = \frac{1}{12} q_{cr} L^2 , \tag{34}$$

For the simply supported beam the critical moment is equal to 454,8 kNm and for the fixed beam 984,3 kNm. For comparison: calculation of the critical moment of a beam of the same cross-section, span and boundary conditions but with no lateral restraint using procedure according to [3] results in M_{cr} = 261,1 kNm (simply supported beam) and M_{cr} = 885,9 kNm (fixed beam). In this case the lateral restraint causes increase of critical moment of about 74 % (simply supported beam) and 11 % (fixed beam).

Application of the QR algorithm results in minimum eigenvalue of 142660 (simply supported beam) and 462393 (fixed beam). Appropriate critical moment determined using (33) is 445,8 kNm (simply supported beam) and using (34) 963,3 kNm (fixed beam). In Fig. 5 three lowest normalized eigenvectors (buckling shapes) of the matrix *G* obtained using QR algorithm are displayed (for clarity reasons higher eigenvectors are not displayed). In Fig. 6 graphical distribution of matrix *G* eigenvalues as a result of the QR algorithm is shown.

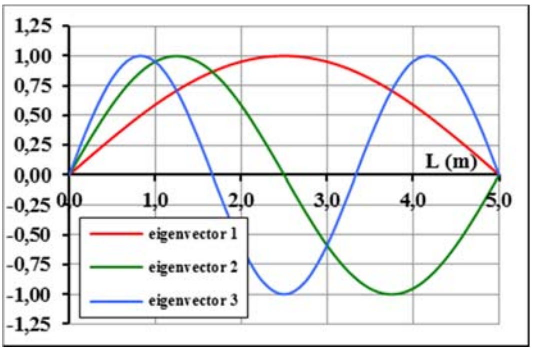

Fig. 5: Three lowest buckling shapes

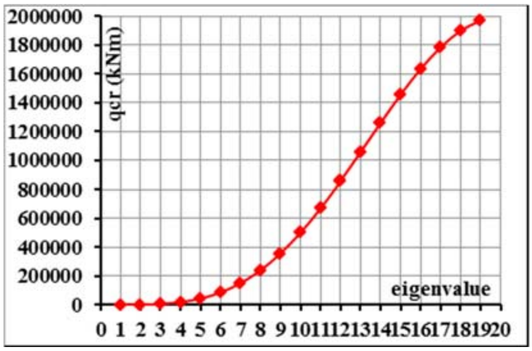

Fig. 6: Eigenvalues of the matrix *G*

3.3 Solution using finite element method and comparison of results

The example mentioned in the section 3.2 is solved using the finite element method code ANSYS 14.0 [9]. The thickness of each part of the cross-section is low in comparison with other dimensions. For this type of constructional members the shell finite elements are suitable. For the analysis the SHELL181 finite element is utilized. The beam cross-section, position of lateral restraint and load is in accordance with the example solved in section 3.2. Two types of support conditions are considered: simply supported beam and fixed beam. For the numerical analysis the finite element edge length 20 mm is specified. The detail of modeled beam including lateral restraint implementation can be seen in Fig. 7 (fixed beam; warping of support cross-section prevented). In case of the simply supported beam the so called fork support condition applies. According to [10] this support condition is considered for lateral torsional buckling analysis. It prevents lateral displacement at supports while warping is allowed. First order theory static analysis and linear buckling analysis (eigenvalue analysis) were performed. It results in minimum positive eigenvalue of 146610 (simply supported beam) and 434338 (fixed beam). Results of critical moments approximations obtained by finite difference method with subsequent inverse power method or QR algorithm, respectively, and finite element method using the ANSYS 14.0 code are summarized in Tab. 1. In Fig. 8 there is one of the results of the numerical analysis using the ANSYS code – first positive eigenvalue for the case of the fixed beam.

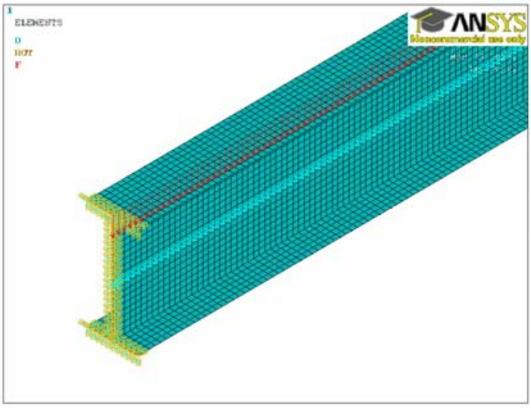

Fig. 7: Finite element model

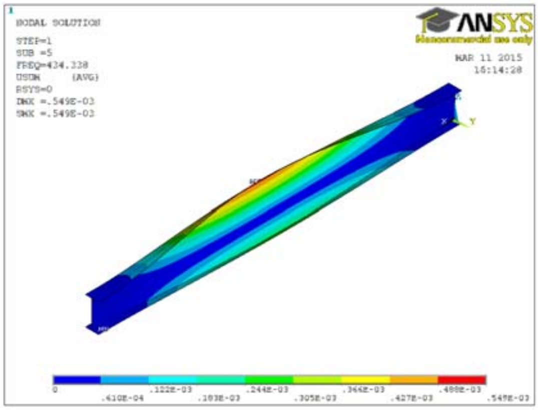

Fig. 8: First positive buckling shape

Tab. 1: Comparison of results – approximations of critical moments (in kNm)

Method	**Beam**	
	simply supported	**fixed**
Finite difference method + inverse power method	454,8	984,3
Finite difference method + QR algorithm	445,8	963,3
Finite element method (ANSYS)	458,2	904,9

3.4 Algorithmisation of the numerical methods for critical load determination and parametric studies

Algorithms of the finite difference method, inverse power method and QR algorithm were programmed in the VBA language (programming language for the MS Excel application). After entering of input data (cross-section characteristics, beam span, position of lateral restraint, position of the load, step *h* of the interval mesh and required accuracy of iterative calculation the code meshes the beam span (discretization of the problem), assembles matrices and vectors and iteratively calculates the minimum eigenvalue.

Following charts show some results obtained by the code. In Fig. 9 there is relationship between eigenvalue and size of the step *h*, Fig. 10 shows convergence of the iterative calculation of the inverse power method to the minimum eigenvalue for different beam span mesh. The convergence is very fast. The input data is identical with the data utilized for the example in section 3.2 for the case of the fixed beam.

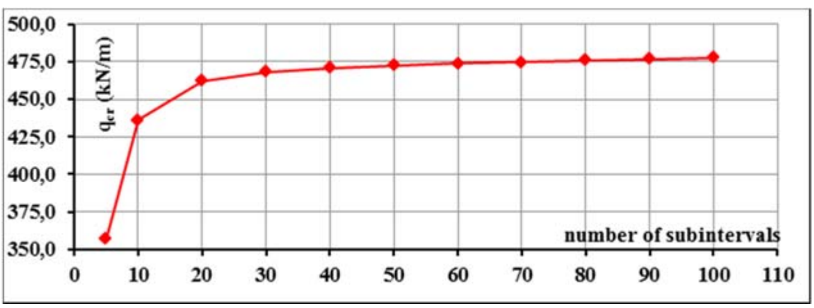

Fig. 9: Relationship between critical load and beam span mesh

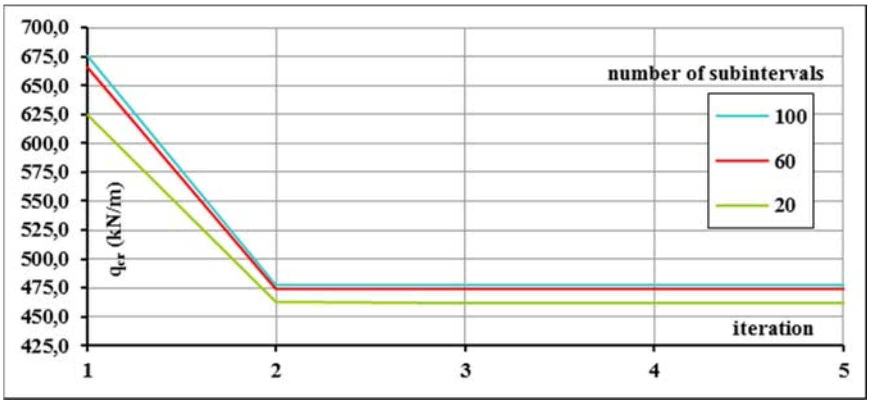

Fig. 10: Convergence of iterative calculation to first positive eigenvalue

Fig. 11 shows comparison of critical loads of a simply supported beam with no lateral restraint (calculation according to [3] and the ANSYS code) and analogous laterally restrained beam (calculation using finite difference method – FDM and the ANSYS code) of various spans. Fig. 12 shows the comparison for a fixed beam (for clarity purposes spans from 5 m to 10 m only are displayed).

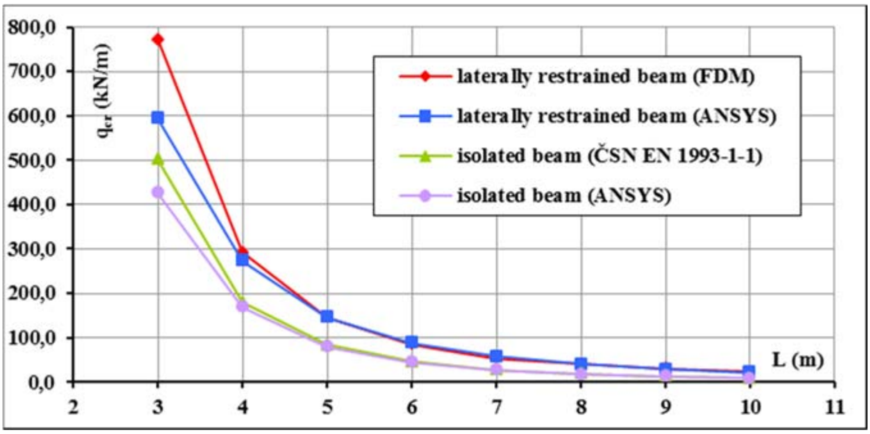

Fig. 11: Comparison of methods of critical load determination – simply supported beam

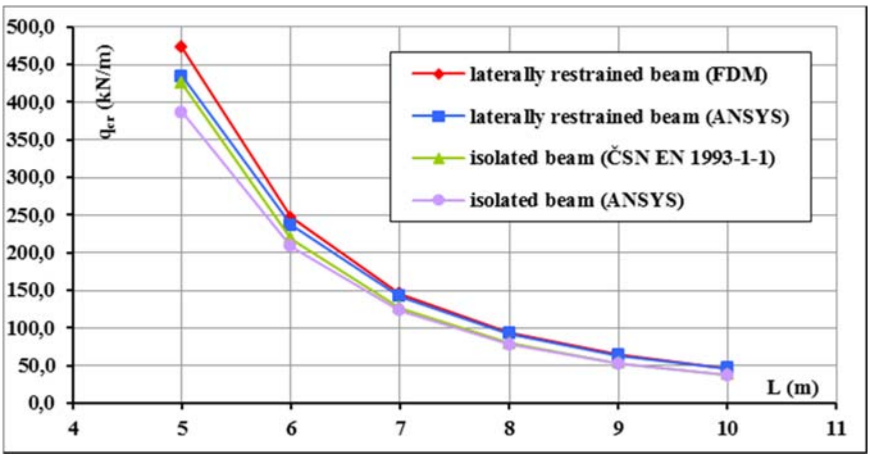

Fig. 12: Comparison of methods of critical load determination – fixed beam

There are certain noticeable differences among values of critical loads for small spans (low slendernesses) of the beams. These differences can be apparently explained by numerical finite element analysis that takes into account also effects of local buckling of thin walls of the cross-sections. These local stability effects act together with global buckling of a beam and influence the resulting values of critical loads. For greater spans the global stability completely prevails and difference between methods is not significant. The system matrix of the finite difference method was derived from the differential equations of global stability of a thin-walled beam (provided the cross-section does not distort). It follows that mentioned local effects are not included.

4 CONCLUSIONS

The paper focuses on lateral torsional buckling of thin-walled beams with lateral continuous restraint. The lateral restraint increases buckling resistance of members; its influence on critical moment was quantified using example of a beam of double symmetric cross-section. The results were compared with results of an analogous beam with no lateral restraint. For the critical load determination selected numerical methods were utilized. A code for computerized calculation in the VBA language was created. It implies from the performed parametric studies that the influence of lateral restraint on critical load is significant. If it is correctly taken into account it might result in more economical cross-section design that positively influences material consumption. Constructional design might be therefore more effective.

The approximations of critical loads were compared with results of numerical analyses performed using a finite element code. Certain differences between results for smaller beam spans are explained by local stability effects that arise from the finite element method analysis.

Described numerical algorithms (finite difference method, inverse power method) are relatively easy to algorithmize and allow to create applications for eigenvalue problems solution.

ACKNOWLEDGMENT

The paper has been supported by the projects of the specific research program of the Brno University of Technology No FAST-J-14-2345 and the Czech Science Foundation No P105/12/0314.

REFERENCES

[1] BŘEZINA, V. *Buckling Resistance of Metal Bars and Beams (Vzpěrná únosnost kovových prutů a nosníků)*. Prague: State Publishing of Technical Literature, 1962. 384 pp.

[2] VLASOV, V. Z. *Thin-Walled Elastic Bars (Tenkostěnné pružné pruty)*. Prague: Czechoslovak Academy of Sciences Publishing, 1962. 572 pp.

[3] ČSN EN 1993-1-1. *Eurocode 3: Design of Steel Structures – Part 1-1: General Rules and Rules for Buildings (Eurokód 3: Navrhování ocelových konstrukcí – Část 1-1: Obecná pravidla a pravidla pro pozemní stavby)*. Prague: Czech Standard Institute, 2006. 96 pp.

[4] RATTANA, A. & BÖCKMANN, C. Matrix methods for computing eigenvalues of Sturm-Liouville problems of order four. *Journal of Computational and Applied Mathematics*. Volume 249, pp. 144–156, ISSN (Online) 0377-0427, DOI: 10.1016/j.cam.2013.02.024, 2013.

[5] KINDMANN, R. & LAUMANN, J. Determination of eigenvalues and modal shapes for members and frames (Ermittlung von Eigenwerten und Eigenformen für Stäbe und Stabwerke). *Stahlbau*. Volume 73, Issue 1, pp. 26–36, ISSN 0038-9145, 2004.

[6] DALÍK, J. *Numerical methods (Numerické metody)*. Brno: CERM Academic Publishing, 1997. 145 pp. ISBN 80-214-0646-1.

[7] VONDRÁK, V. & POSPÍŠIL, V. *Numerical methods I (Numerické metody I)*. [online]. 2011. http://mi21.vsb.cz/sites/mi21.vsb.cz/files/unit/numericke_metody.pdf.

[8] BJORCK, A. Numerics of Gram-Schmidt orthogonalization. *Linear Algebra and its Applications*. Volume 197-198, pp. 297–316, ISSN (Online) 0024-3795, DOI: 10.1016/0024-3795(94)90493-6, 1994.

[9] ANSYS® Academic Research, Release 14.0.

[10] SEDLACEK, G. & NAUMES, J. *Excerpt from the Background Document to EN 1993-1-1: Flexural buckling and lateral buckling on a common basis: Stability assessments according to Eurocode 3*. Aachen: Institut und Lehrstuhl für Stahlbau und Leichtmetallbau, 2008. 142 pp.

Reviewers:

Doc. Ing. Martin Psotný, PhD., Department of Structural Mechanics, Faculty of Civil Engineering, Slovak University of Technology in Bratislava, Slovak Republic.

Prof. Ing. Josef Vičan, CSc., Department of Structures and Bridges, Faculty of Civil Engineering, University of Žilina, Slovak Republic.